

FINAL REPORT

BEHAVIOR OF PLASTIC SAND CONFINEMENT GRIDS

N.F. Coetzee
Engineering Research Center
Institute of Northern Engineering
University of Alaska-Fairbanks
Fairbanks, AK 99775

January 1986

ALASKA DEPARTMENT OF TRANSPORTATION AND PUBLIC FACILITIES
RESEARCH SECTION
2301 Peger Road
Fairbanks, AK 99701

The contents of this report reflect the views of the authors who are responsible for the facts and the accuracy of the data presented herein. The contents do not necessarily reflect the official views or policies of the Alaska Department of Transportation and Public Facilities. This report does not constitute a standard, specification or regulation.

TABLE OF CONTENTS

	<u>Page</u>
Introduction.....	1
Pavement System.....	4
Finite Element Analyses.....	5
Elastic Layer Analyses.....	17
Conclusions and Recommendations.....	18
References.....	21
Appendix.....	24

INTRODUCTION

The concept of improving the load carrying ability of unbound aggregates, particularly sand, by lateral confinement has been investigated for some time (1,2,3,4). Extensive full-scale testing of the trafficability of confined beach sand pavement layers has been carried out by the U.S. Army Corps of Engineers at the Waterways Experiment Station (WES) in Vicksburg, Mississippi. Confinement is achieved using a honeycomb type of grid cell structure developed by the Corps and constructed of various materials (1, 2). Initial material types included paper and aluminum, with the current, and apparently most successful, confinement grids made of high density polyethylene (HDPE) produced and marketed by Presto Products (PTY) Ltd. The grid configuration in the expanded form is shown in Figure 1. Actual grid panel dimensions and material properties are listed in Table 1, based on information provided by the manufacturer. The experimental work by the Corps had as its primary objective the determination of structural adequacy of pavements for temporary facilities. However, there are apparent advantages in using the sand confinement approach in permanent installations, as base or subbase layers, where suitable aggregate material is not available, or is costly to obtain. This situation exists particularly in western Alaska where often the only construction material that is readily available is sand, so aggregate, if used, is imported at a high cost. The alternative to imported material is the use of sand stabilized with asphalt. This usually provides the surfacing layer. Use of the Presto plastic sand confinement grid may provide an economically attractive alternative as the base or subbase layers for a pavement structure in this area.

A product evaluation was performed for Alaska Department of Transportation and Public Facilities (DOT&PF) in 1983 and published as Report No. AK-RD-84-8 (1). Results from the evaluation indicated that finite element and elastic layer analyses of a pavement structure containing grid reinforced layers could provide useful design information, but that the analyses performed for the evaluation required

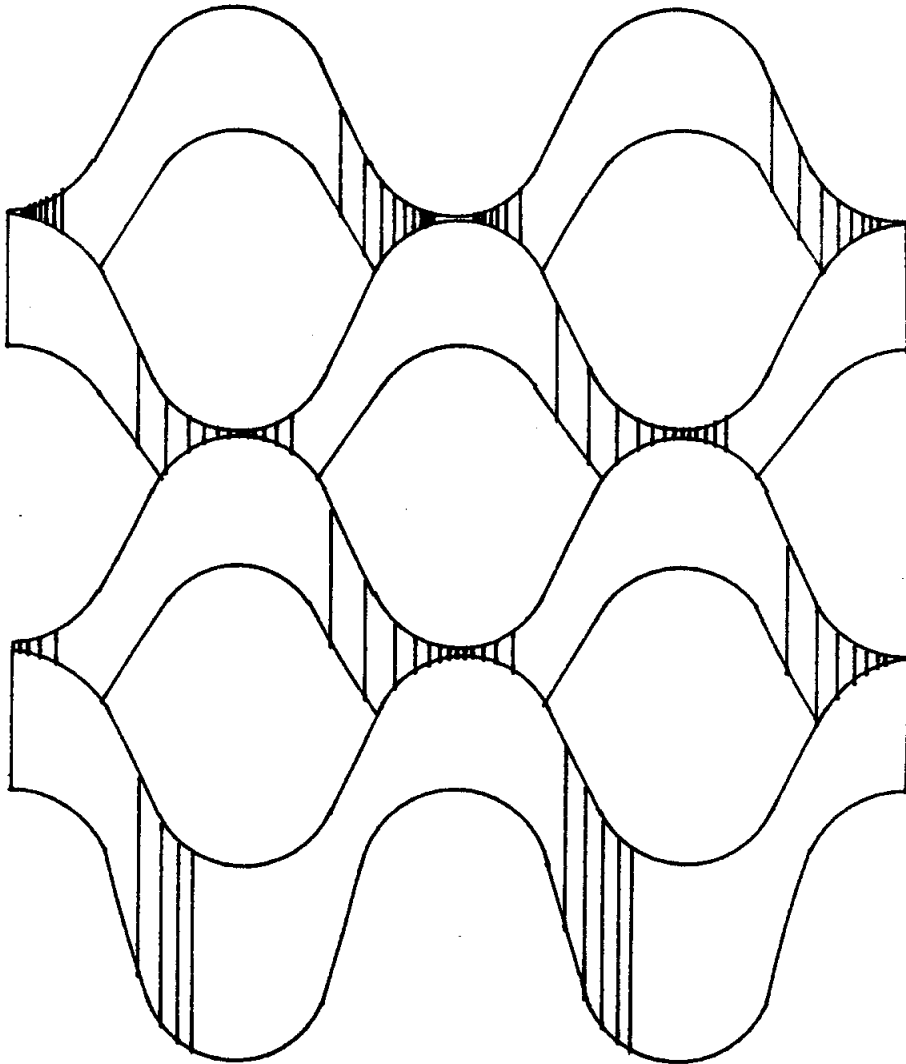


Figure 1. Expanded configuration of GEOWEB sand confinement grid.

TABLE 1. Presto GEOWEB Grid Information (4).

MATERIAL:	HDPE	
YOUNG'S MODULUS (E):	Approximately 100,000 psi	
ULTIMATE STRENGTH AND ASSOCIATED STRAIN:	σ_u (psi)	ϵ (%)
Machine direction (i.e., in direction of extrusion)	3,650	455
Transverse direction (i.e., normal to extrusion direction)	3,605	238
EXPANDED PANEL SIZE:	8 ft x 20.5 ft x 8 in	
FOLDED PANEL SIZE:	13 ft x 11 in x 8 in	
SHEETS OF HDPE/PANEL:	60	
NO. OF CELLS/PANEL:	561	
APPROX. CELL AREA (EXPANDED)	0.274 ft ²	
HDPE THICKNESS:	0.055 in	
SHIPPING WEIGHT/PANEL	122 lb	

a certain amount of refinement. This report covers the results obtained from such refined analyses of pavement response to high wheel loads in terms of the effects on grid confined layers. Finite element and elastic layer analysis results are presented and compared with the earlier results.

PAVEMENT SYSTEM

The same pavement structure was analyzed as in the earlier evaluation, for comparison purposes, and is shown in Figure 2.

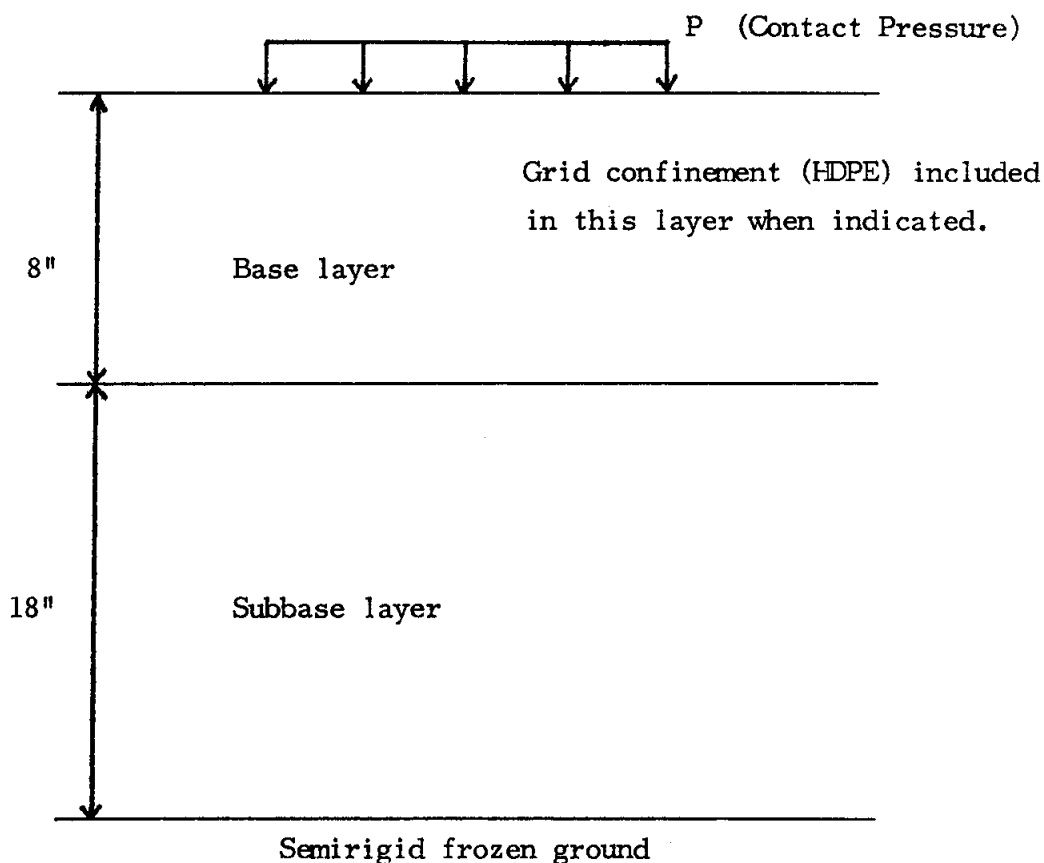


Figure 2. Idealized pavement structure used in analyses.

Figure 2 adequately describes the system analyzed by elastic layer methods. Applied wheel loads were based on the Lockheed L-382 Hercules aircraft at maximum gross takeoff weight, with a modification made to the contact pressure used in the finite element analysis, based on the geometry of the pavement simulation, so that the total load carried by the pavement remained constant at 36,800 lbs. This aircraft was chosen since it represents the most probable maximum wheel loads at Shishmaref. Figure 3 shows schematically the pavement system that was used in the three dimensional finite element analyses. Boundary conditions shown in Figure 3 were based on considerations of symmetry, since the analysis considered one wheel only.

FINITE ELEMENT ANALYSES

The computer program SAP IV (8) running on a VAX 11/730 was used for all the finite element analyses. As in the previous work (1), the confined material was modeled by three dimensional solid elements whereas the confining material (i.e., grid) is represented by truss elements. The arrangement is shown schematically in Figure 4, of an 8-node solid (brick) element, with the element corner node displacements restrained by the solid element material as well as the truss framework. Analyses were performed using both the 8-node brick and the 17-node thick shell elements shown in idealized form in Figure 5 (8). All refinements over previous analyses concentrated on the grid confined layer only (i.e., the upper layer) shown in Figures 2 and 3, and involved reduced element thickness for the 8-node brick, use of the 17-node thick shell element instead of the brick element, and a single case of higher integration order for the thick shell element. Plan dimensions of the solid elements were maintained at a 6" x 6" square configuration throughout, as in the earlier analyses (1). The dimensions were based on the surface area of a grid cell in the expanded GEOWEB section. The specific analyses performed included:

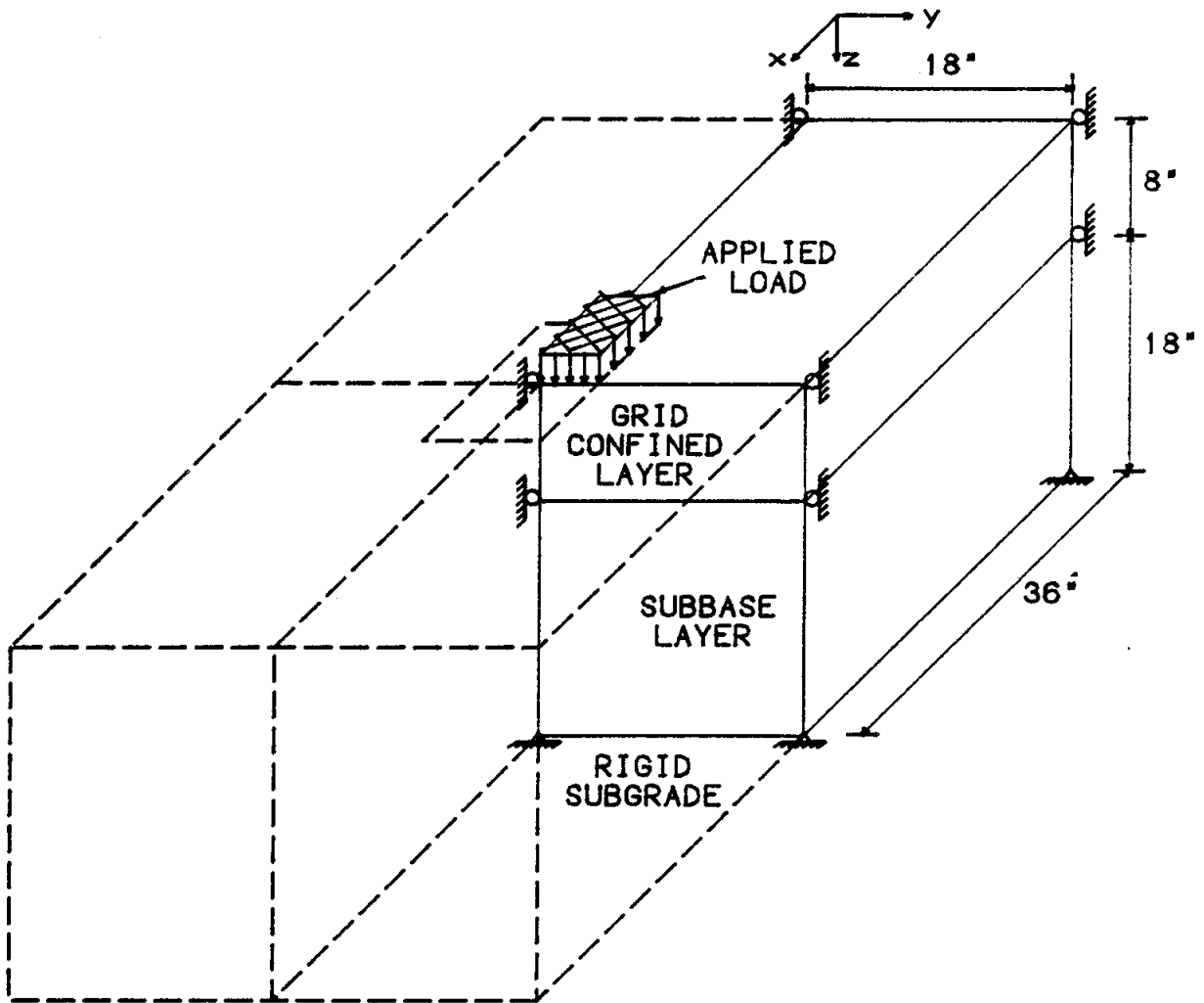
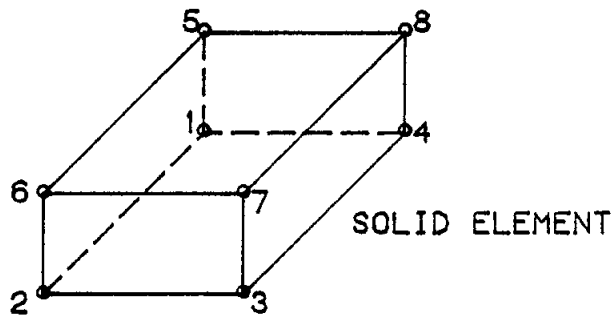


Figure 3. Schematic of the pavement system used in the three-dimensional finite element analyses.



PLUS

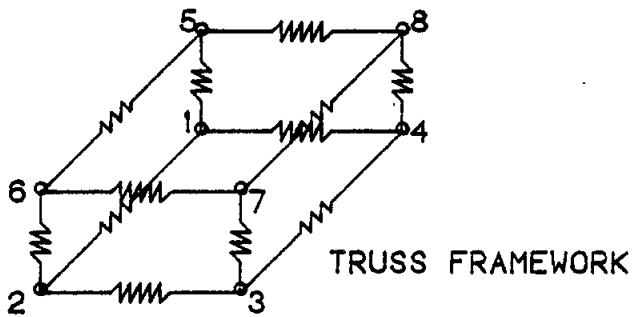
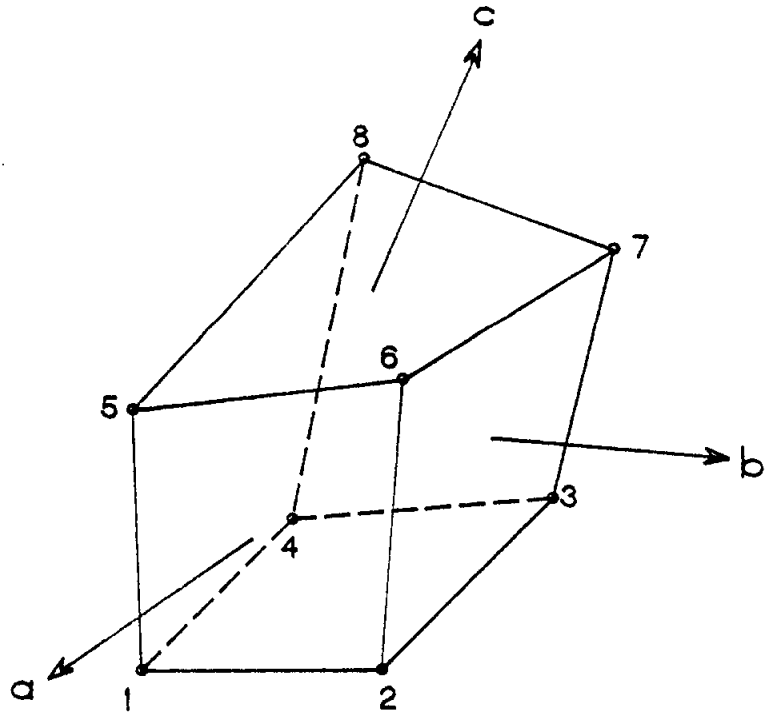
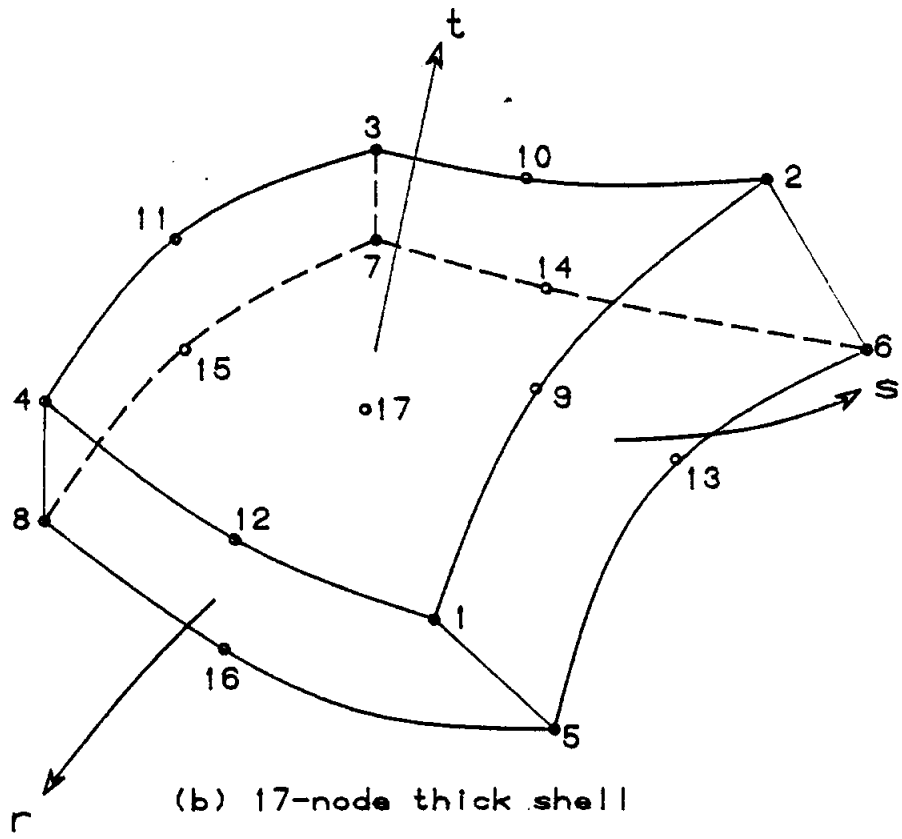


Figure 4. Element combinations used to represent confined material.



(a) 8-node brick



(b) 17-node thick shell

Figure 5. Solid elements used in analysis.

1. Use of 8-node brick element in a finer mesh to simulate confined material. Thickness is reduced to 1" so that there are eight layers of these elements in the grid confined layers. Truss elements are sized accordingly.
2. Use of two layers of 4" thick 17-node elements to simulate the grid confined layers. This does provide output at depth increments of 2" due to the presence of the 17th node at the centroid of the element.
3. As for 2 but with four layers of 2" thick elements.
4. A single computer run using an integration order of four rather than the default value of two for the 17-node elements.

Material characteristics for the analyses were based on assumed values from the literature (2,5,9,10,11) as well as measured values for the Shishmaref sand (13), and duplicated the values used in the previous analyses. These values are listed in Table 2.

TABLE 2. Material characteristics used for analyses.

Material	HDPE grid	Confined sand	Unconfined sand subbase	Frozen subgrade
Young's Modulus E (psi)	100,000	20,000	varies	rigid
Poisson's ratio	0.3	0.4	0.4	0.4

Subbase modulus values of 5,000, 10,000, 15,000 and 20,000 psi were used to simulate the possible variations that may occur in the field as a result of varying moisture content and drainage characteristics. The low modulus would be expected during spring thaw when frozen lower strata prevent drainage of the thawed and saturated upper layers.

Analyses of unconfined systems were not performed, since, as was found in the original analyses, the low volume ratio (<2%) of high modulus material in the confined layer results in fairly small differences in idealized elastic behavior between the two systems.

Results of the analyses using the 2" thick 17-node element were used to plot the stress distributions in the confined layers shown in Figures 6 through 9. The stress distribution for the solid element is based on values provided by the SAP program at the centroid of the most highly stressed elements, which occur directly beneath the load. The distribution appears reasonable, with, for instance, vertical compressive stresses at the surface of the layer approximating the applied load pressure of 130 psi, and decreasing with depth.

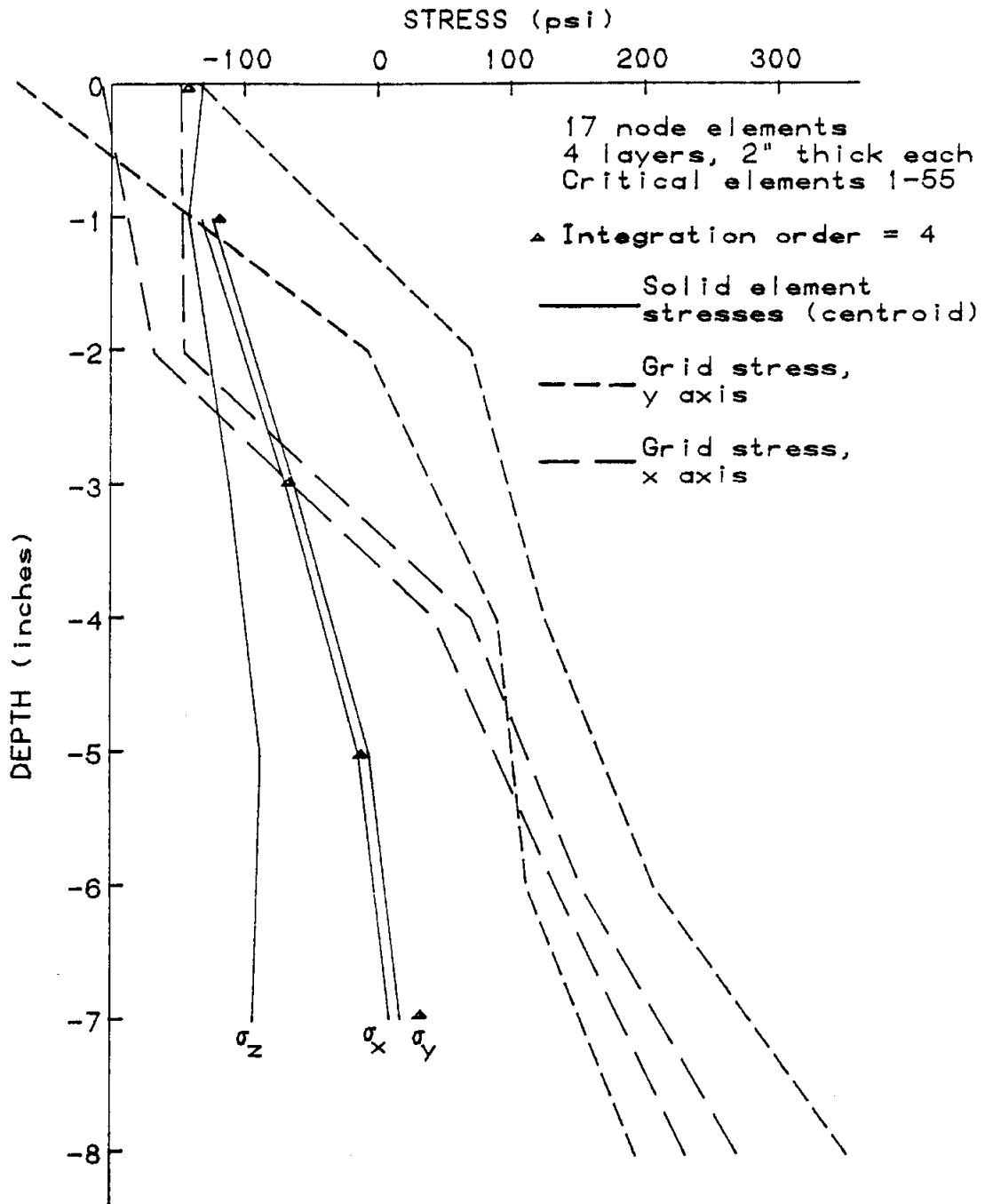
Also shown in these figures are the maximum grid tensile stress values as calculated by SAP, with a maximum value of approximately 350 psi tension for a subbase modulus of 5,000 psi (Figure 6) to a minimum of approximately 140 psi for a subbase modulus of 10,000 psi. The difference in stress between the x and y directions results from the choice of dimensions for analysis resulting in a nonaxisymmetric analysis. Inspection of Figure 6 shows that some tension is being

carried by the solid element. Since this element is simulating the sand in the confined layer, it can, in fact, carry only compressive loads, so tensile stresses need to be transferred to the grid reinforcement which is the only system component in the confined layer capable of carrying tension. Details of the approach used for the stress transfer calculations are provided in the Appendix.

It should be noted that the procedure provides at best a reasonable estimate of actual grid stresses, and introduces incompatible nodal displacements between grid and sand. Ideally, the procedure should be incorporated into the finite element analysis by use of nonlinear material behavior, which would produce more realistic results. Programs capable of doing this are available but usually require substantial computer time due to the iterative process involved, especially in three dimensions. In performing the stress transfer calculations, tensile stresses at the edges of the solid element were transferred to the grid since this is the physical location of the grid relative to the solid element. This is a conservative approach since the edge stresses are extrapolated, by the computer program, and are in all cases higher than the centroid stresses.

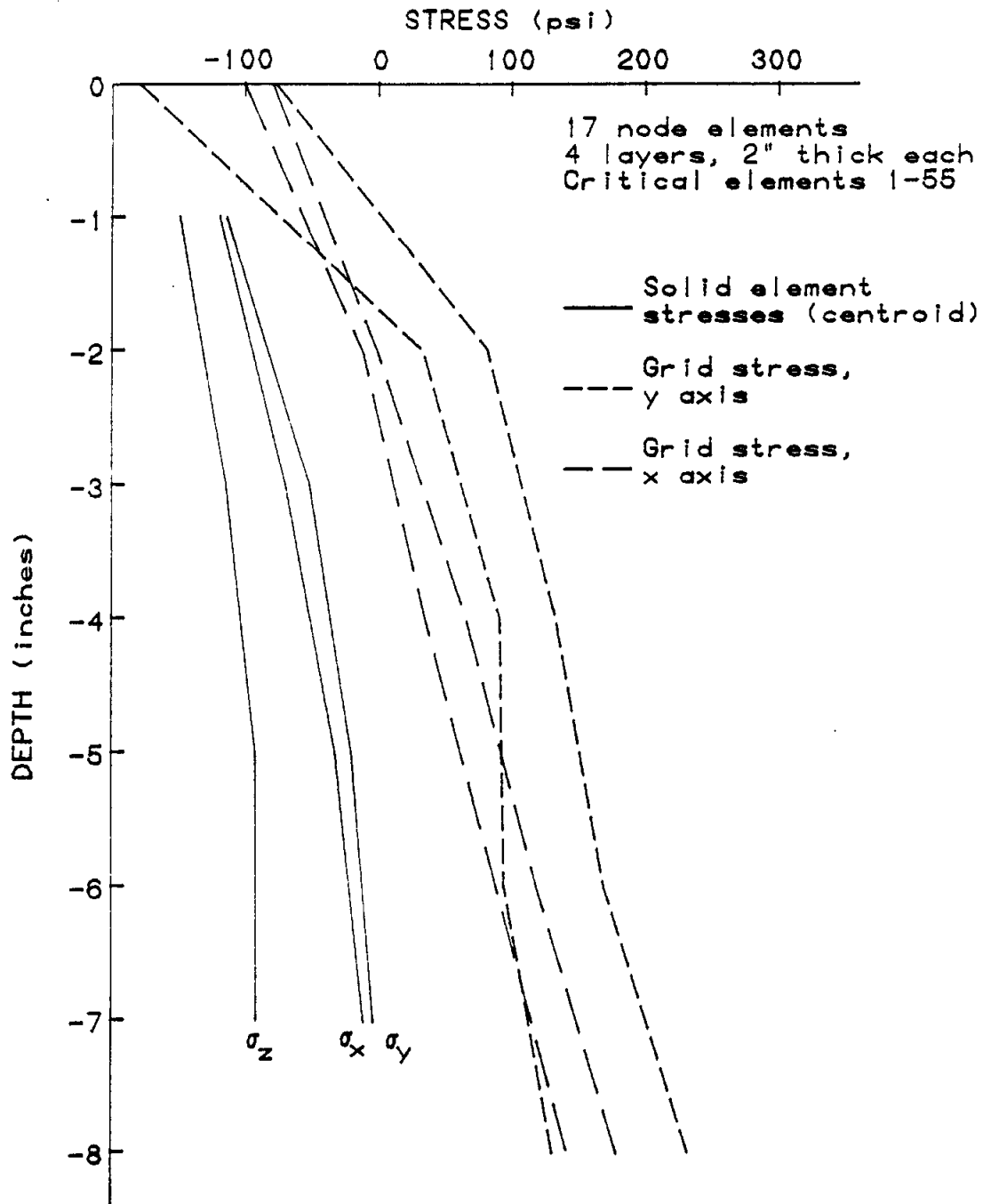
For example, Figure 7 shows both horizontal stresses at the centroid of the solid element to be compressive, while, as can be seen in the Appendix, tensile stresses on the edge of the same solid element are as high as 17.8 psi. The transferred stresses are plotted in Figure 10, as well as the originally calculated grid stresses. As can be seen from Figure 10, the transfer of all tension to the grid can result in a very large increase in grid stress: e.g., from about 240 psi, as calculated by SAP, to an estimate of 2,992 psi in the worst case. This is to be expected, since the volume ratio of grid to sand is 0.0193, so that transfer of 1 psi of tension from the sand results in $1/0.0193$ or 51.8 psi added to the grid.

Note that this approach is significantly different from that used in the original analyses for stress transfer, which attempted to calculate the total tensile force carried by the solid element and then transfer this force to the grid. The complexity of stress distributions within an element make this, at best, a difficult procedure. The current approach is much simpler since stress estimates are made at a



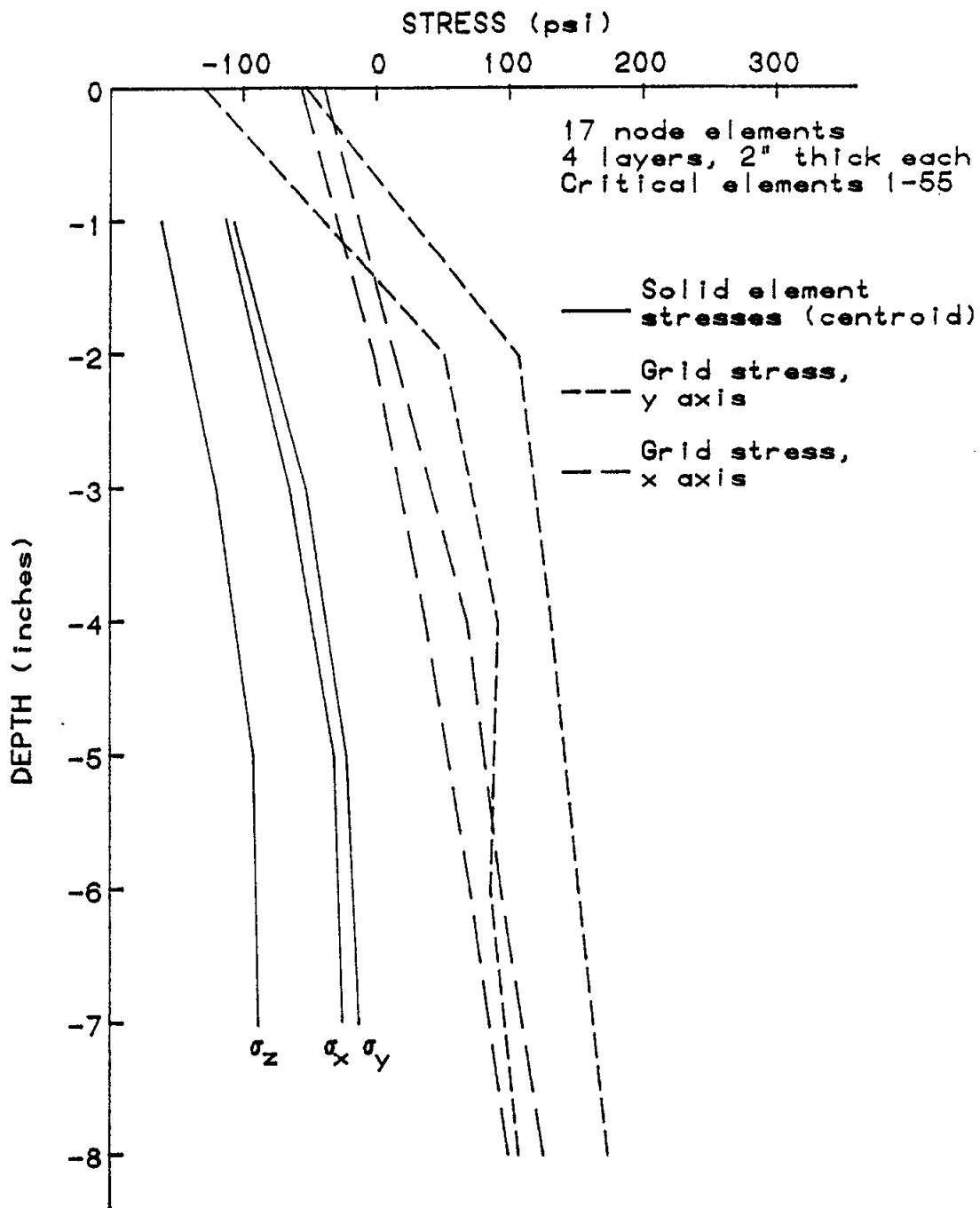
NOTE: Bounds on grid stresses in x,y directions defined by grid elements on either side of critical solid elements

Figure 6. Stress distributions within the confined area ($E_{sg} = 5,000$ psi).



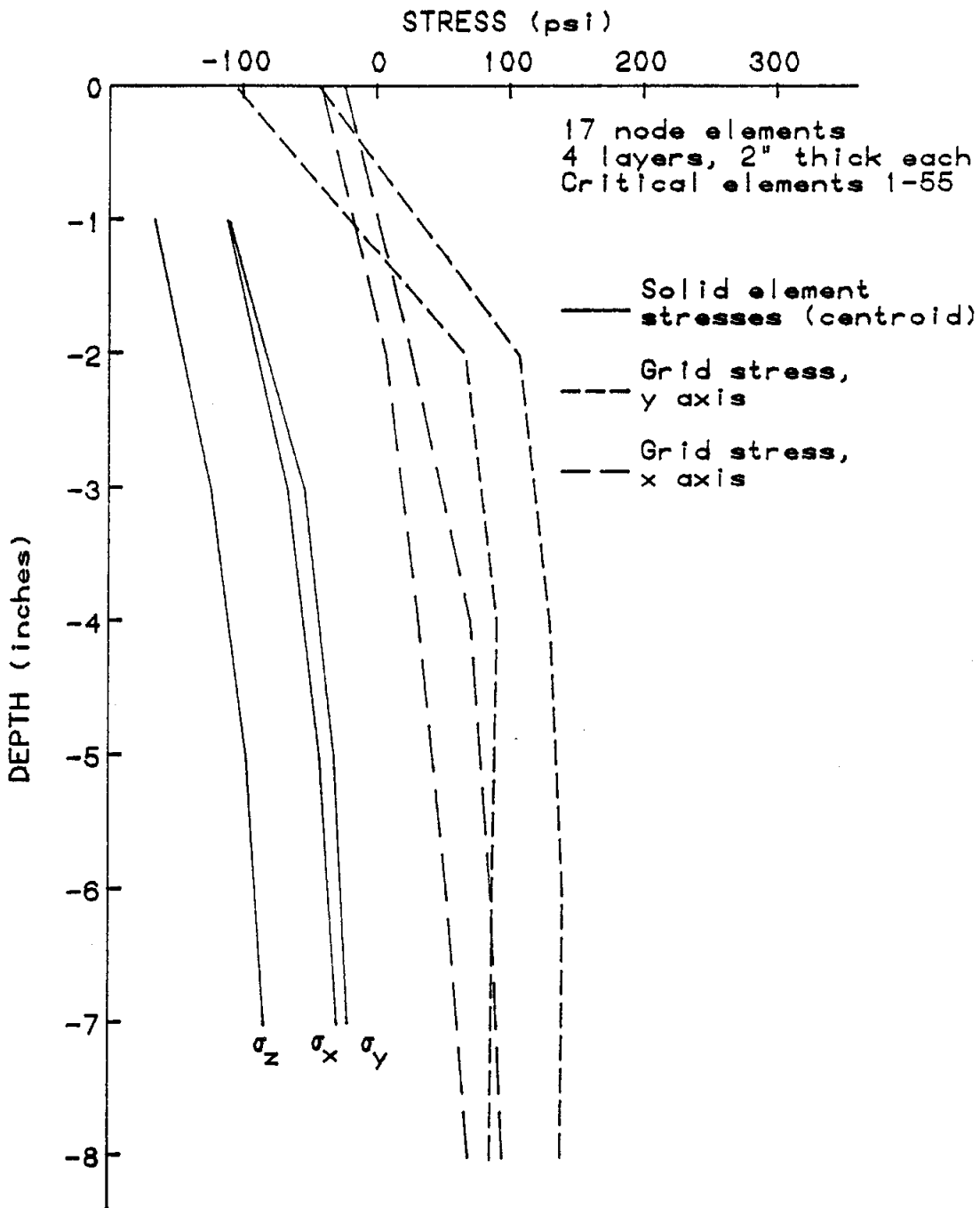
NOTE: Bounds on grid stresses in x,y directions defined by grid elements on either side of critical solid elements

Figure 7. Stress distributions within the confined area
($E_{sg} = 10,000$ psi).



NOTE: Bounds on grid stresses in x,y directions defined by grid elements on either side of critical solid elements

Figure 8. Stress distributions within the confined area ($E_{sg} = 15,000$ psi).



NOTE: Bounds on grid stresses in x,y directions defined by grid elements on either side of critical solid elements

Figure 9. Stress distributions within the confined area ($E_{sg} = 20,000$ psi).

point in the structure where component stresses have been calculated by the finite element program. As a result, it is also probably more accurate from a theoretical point of view, although -- due to the nature of the grid material, which tends to creep under stress so that maximum values tend to be attenuated -- the estimates should be considered conservative and indicative of relatively fast loading rates.

From Figure 10, it can be seen that the fine mesh 8-node element analysis results in the highest transferred stresses for the finite element analyses. The most significant variation occurs at a subbase modulus of 15,000 psi where this analysis indicates significant tension whereas the others do not. The 17-node 4" thick element system appears to substantially underestimate tension in the solid elements. The 17-node 2" thick element system is probably the most reliable system that was used for the analyses. This system shows a range of grid tension (at a subbase modulus of 5,000 psi) from 2,500 to 3,000 psi. By increasing the integration order, this range was reduced to 2,250-2,600 psi which would be a more accurate estimate than at the lower integration order, at a slight additional cost in computing time.

Compared to earlier analyses, at the low subbase modulus values the estimated grid stresses are about twice as high as previously estimated. This is a result of a combination of refined element and mesh use, and the altered method of stress transfer which does not average any stresses but determines maximum value at a point. Although the maximum estimated grid stresses are still below the ultimate strength of the grid material (3,500 psi), the high strains required for stresses of this level (3,000 psi) would constitute failure of the grid system except, possibly, under very rapid loading conditions. However, creep of the HDPE would redistribute these stresses to acceptable levels with some rutting occurring in the wheel paths.

ELASTIC LAYER ANALYSIS

In an attempt to simplify estimation of grid stresses under wheel loads, elastic layer programs were used to analyze the structure shown in Figure 2. These programs require very little data preparation as

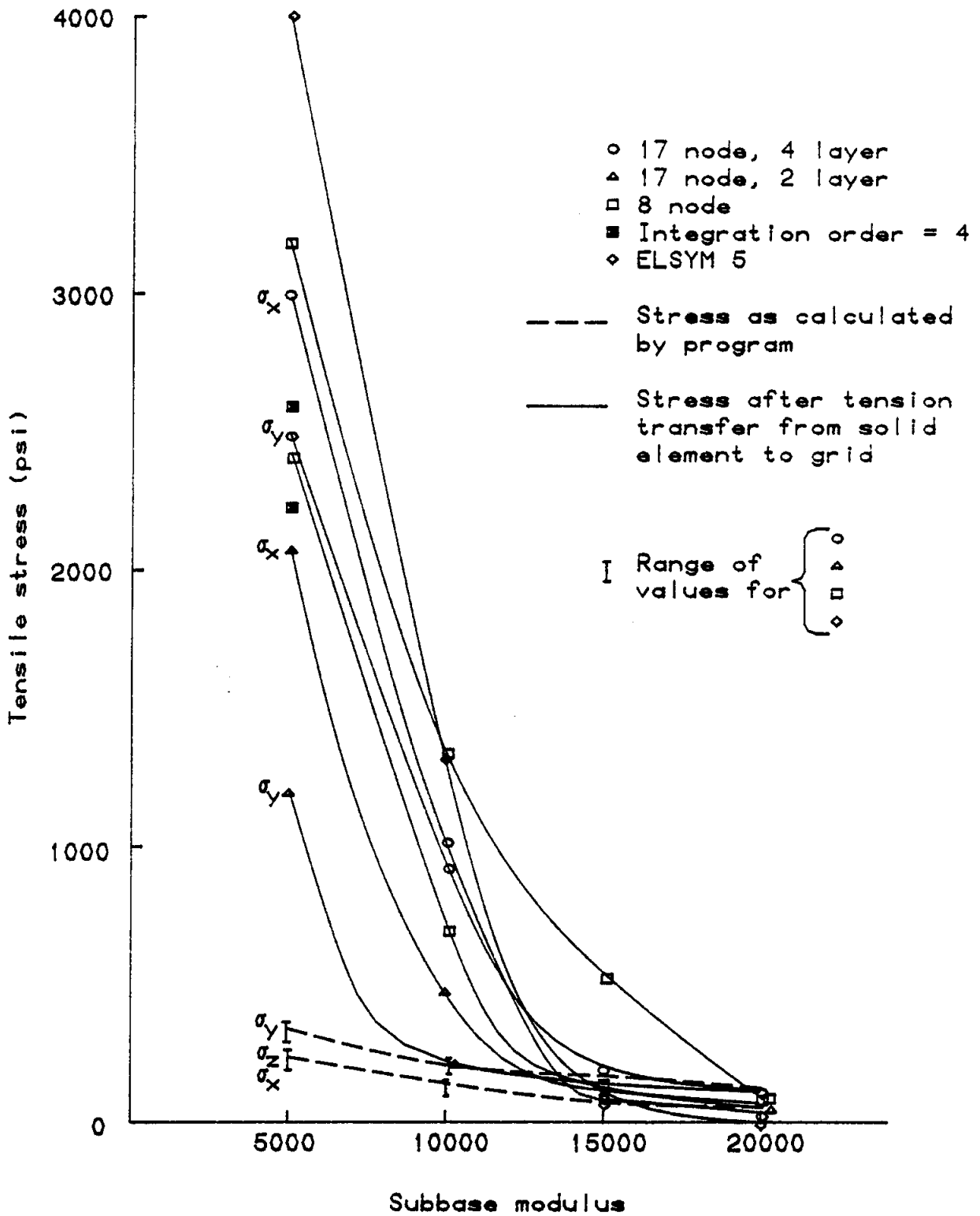


Figure 10. Variation of maximum grid stress with subbase modulus.

compared to finite element analyses, but assume that each layer is infinite in the horizontal plane and that the material is homogeneous and isotropic, so that the grid confined system cannot be modeled directly. In the original analyses, the grid was transformed into two equivalent horizontal layers of HDPE. The question arises as to how many layers should be used, and where they should be placed. It seems that the most reasonable approach is to consider the grid material as being "smeared" throughout the confined layer. In effect, the confined layer is considered homogeneous with properties based on a simple mixture rule, as is often done in the macroscopic study of composite materials. The confined layer is given a composite modulus E_c defined by

$$E_c V_c = E_g V_g + E_s V_s$$

where

E = elastic modulus

V = volume

with subscripts c = composite

g = grid

s = sand

The data listed in Tables 1 and 2, when used in this relationship, provide a composite modulus of 21,515 psi. ELSYM5, one of the elastic layer programs, was used to analyze the structure shown in Figure 2 using this value of modulus for the confined layer and varying the subbase modulus between 5,000 and 20,000 psi as for the finite element analyses. The frozen subgrade modulus was assumed to be 400,000 psi (12). The variation in horizontal stress within this composite layer is shown in Figure 11. Based on the ELSYM5 analyses, some tension occurs in the bottom of the confined layer, at a higher subbase modulus (15,000 psi) than for the finite element analysis. In the finite element analyses, no tension occurred and hence no transfer was required for a subbase modulus greater than 10,000 psi, except in the 8-node element approach. This results from the truss elements carrying all tension at the higher subbase moduli.

For the elastic layer results, using the same argument as before, all tension needs to be transferred to the grid. The same transfer approach is used, except that now the ratio of grid volume to total volume is used to calculate grid stress (i.e., 0.0189 instead of 0.0193) since the grid has not been included explicitly in the system, as it was in the finite element analyses.

The transfer calculations are shown in the Appendix, and the results plotted on Figure 10. This approach results in substantially higher grid stress estimates than the finite element analyses, with a maximum of 4,029 psi at a subbase modulus of 5,000 psi.

CONCLUSIONS AND RECOMMENDATIONS

1. Conclusions based on the earlier analyses that still stand are as follows.
 - A. Bearing capacity analysis indicates that the confining grid system substantially increases the ultimate capacity of cohesionless material if one considers the effect of the grid to be that of introducing an apparent cohesion. This covers the situation where failure involves the lateral and upward displacement of the loaded material. Bearing capacity considering the grid layer as a surcharge should also be considered.
 - B. Neither the finite element nor the elastic layer solutions model the behavior of cohesionless material in an exact manner since it is assumed that the elastic modulus in tension is the same as in compression. Analyses involving grid confinement material were modified by assuming that all tensile stress in a confined layer is transferred to the grid, resulting in zero tensile stress on the cohesionless material. The approach leads to strain incompatibility in the confined layer and should be further investigated to ensure that the resulting stress and strain distribution is reasonable.

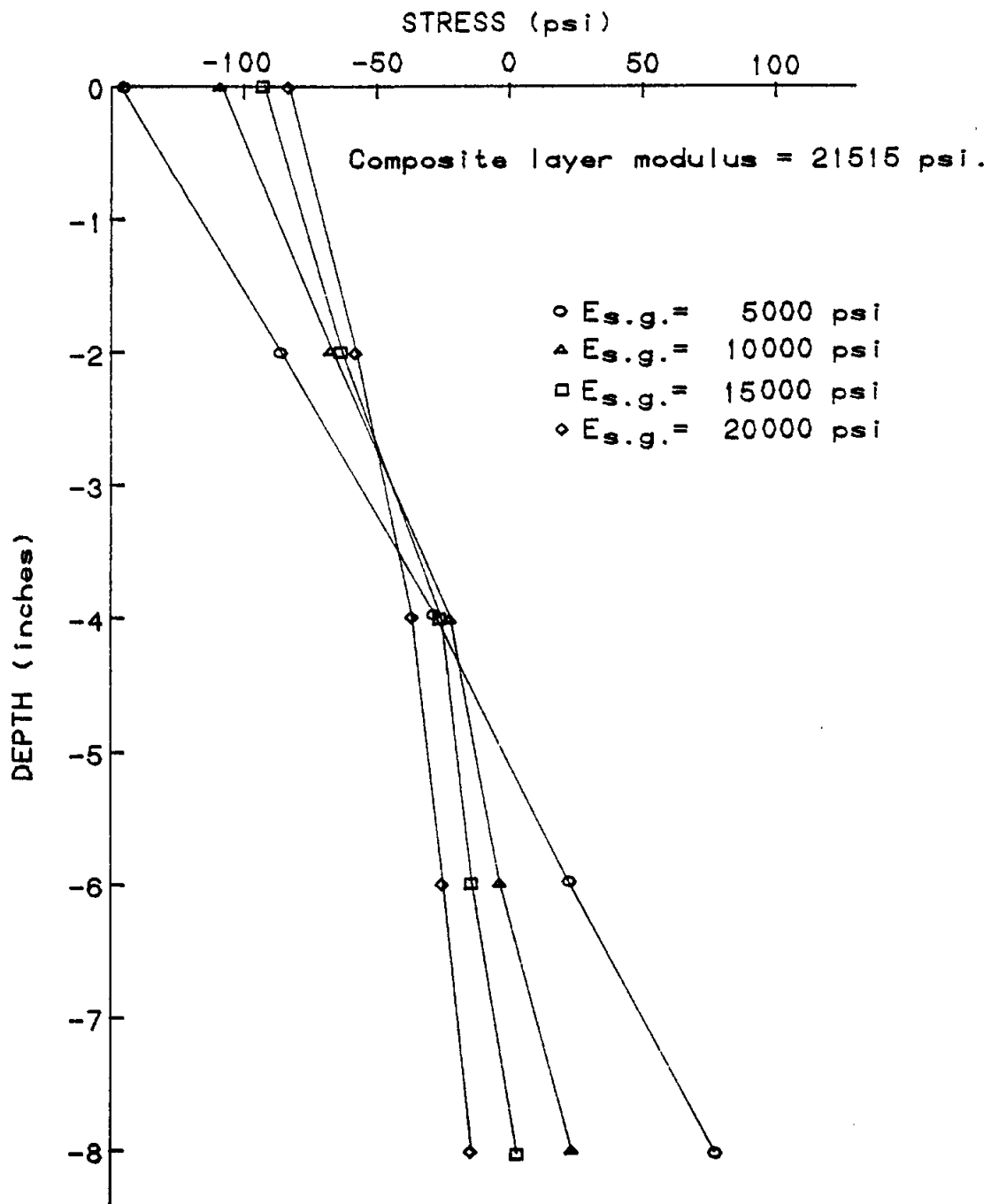


Figure 11. Horizontal stress distribution within composite layer using ELSYM5.

- C. Analyses of a system with and without the grid confinement show little difference in stress distributions between the confined and unconfined system due to the low volume percent of confining material involved and the assumption of linear elastic behavior. However, if tensile stresses are transferred from cohesionless materials to the grid, the confined system exhibits a significantly improved response to load, due to its ability to carry tension in the confined layer.
- D. No thermal considerations were included in this evaluation. The behavior of the grid confining system at low temperatures needs to be investigated.
- E. Laboratory tests on the engineering properties of the HDPE should be conducted at various temperatures to provide suitable design information, particularly since the joint weld strengths are likely to govern performance. This evaluation is based on the assumption that weld strengths of the grid are similar to the HDPE strengths.
2. The current analyses used a simplified approach to stress transfer. The results are probably conservative, but are based on point values provided by the computer analysis, with no additional averaging.
3. Finite element analyses can be used to adequately model the system. A three dimensional nonlinear analysis with tension cutoff for the solid elements (i.e., solid elements unable to carry tensile stress) is likely to give the best simulation.
4. Use of a thick shell element for modeling the solid elements is recommended. Higher integration orders will improve results. Choice of element size is important.

5. Use of elastic layered analysis may provide overconservative results. It is recommended that the composite approach be used, if this method is applied, since choosing number and position of equivalent reinforcement layers introduces the possibility of large variations in estimated stress with the elastic layered approach.
6. The finite element analysis is preferred over elastic layer solutions since the system can be modeled more realistically. However, even with finite element analysis, verifications of predicted stresses and strains are impossible until field measurements are made. Work is currently underway to verify the technique using strain gauge and deflection measuring techniques.

REFERENCES

1. Coetzee, N.F. "Product Evaluation Presto Roadbase Sand Confinement Grid." June 1983. Alaska Department of Transportation and Public Facilities, Fairbanks. Report No. AK-RD-84-8.
2. Webster, S.L. "Investigation of Beach Sand Trafficability Enhancement Using Sand Grid Confinement and Membrane Reinforcement Concepts. Report 1: Sand test sections 1 and 2, November 1979. Report 2: Sand test sections 3 and 4, February 1981." Geotechnical Laboratory. U.S. Army Engineer Waterways Experiment Station, Vicksburg, MS. Technical Report GL-79-20.
3. Burns, C.D. "Traffic Tests of Expedient Airfield Construction Concepts for Possible Application in the National Petroleum Reserve Alaska (NPRA) Geotechnical Laboratory." March 1979. U.S. Army Waterways Experiment Station, Vicksburg, MS. Technical Report GL-79-2.
4. Mitchell, J.K, Kao, T-C., and Kavazanjian, E. "Analysis of Grid Cell Reinforced Pavement Bases." July 1979. Monitored by:

Geotechnical Laboratory, U.S. Army Waterways Experiment Station,
Vicksburg, MS. Technical Report GL-79-8.

5. Weber, C., and Bach, G. Personal communications and Presto Roadbase advertising brochure. August 1982 - April 1983.
6. Raad, L. "Reinforcement of Transportation Support Systems Through Fabric Prestressing." 1980. National Science Foundation, Washington, DC. T.R.B. Transportation Research Record 755.
7. Monismith, C.L., Mitchell, J.K., and Raad, L. "Analyses of Paving Applications of Nonwoven Fabrics." 1977. Prepared for the International Paper Company. Department of Civil Engineering, University of California, Berkeley.
8. Bathe, K.J., Wilson, E.L., and Peterson, F.E. "SAP IV. A Structural Analysis Program for Static and Dynamic Response to Linear Systems." 1974. Earthquake Engineering Research Center, University of California, Berkeley. Report No. EERC73-11.
9. Yoder, E.J., and Witczak, M.W. "Principles of Pavement Design." 1975. John Wiley and Sons, Inc., NY. 711 pp.
10. Hicks, R.G., and McHattie, R.L. "Use of Layered Theory in the Design and Evaluation of Pavement Systems." 1982. Alaska Department of Transportation and Public Facilities, Fairbanks. Report No. FHWA-AK-RD-83-8.
11. Alaska Department of Transportation and Public Facilities (1981) and Fox, J. (1958-1960). Various soils reports and letters relating to Shishmaref materials.
12. Johnson, P. "Operating Vehicles on a Floating Ice Sheet." 1980. Fairbanks, Alaska.

13. Baldassari, D. Memo to B. Connor with test results on Shishmaref Bage and Borrow samples. June 28, 1985. File No. F21821.

APPENDIX
STRESS TRANSFER CALCULATIONS AT BOTTOM OF CONFINED LAYER

I. FINITE ELEMENT

$$\begin{aligned}\text{Vol. HDPE/8'x20' panel} &= 11' \times 8" \times 0.055' \times 60 \text{ sheets} \\ &= 2.017 \text{ ft}^3 \\ \text{Vol. of expanded panel} &= 8 \times 20 \times \frac{8}{12} = 106.667 \text{ ft}^3 \\ \text{i.e., \% HDPE} &= 1.891\% \\ \text{Vol. ratio } \frac{\text{HDPE}}{\text{sand}} &= \frac{2.017}{106.667 - 2.017} = 0.0193\end{aligned}$$

NOTE: this is the same value if areas at any x-section is considered and the HDPE area is corrected for the grid expansion.

In the unexpanded grid, area HDPE

$$\begin{aligned}&= 0.055" \times 8" \times 60 \text{ sheets} \\ &= 26.4 \text{ in}^2\end{aligned}$$

In the expanded configuration, the 60 11 ft sheets are distorted so that they lie in an 8 ft section (i.e., the HDPE area at any section is modified by rotation of the HDPE section) so that a corrected area of

$$\frac{11}{8} \times 26.4 = 36.3 \text{ in}^2$$

occurs in the section and

$$\frac{\text{HDPE}}{\text{sand}} = \frac{36.3}{(20 \times 12 \times 8) - 36.3} = 0.0193$$

Thus, to calculate the transfer stress σ_t use

$$\sigma_t = \frac{\sigma_s}{0.0193}$$

where

$$\sigma_s = \text{sand stress}$$

and then total grid stress σ_{tg} becomes

$$\sigma_{tg} = \sigma_g + \sigma_t$$

where σ_g = grid stress from SAPIV. Total grid stress σ_{tg} is calculated at critical points; usually at bottom of confined layer.

A. 17-NODE 2" THICK ELEMENTS (i.e., four layers of elements in confined layers)

- 1) Subbase modulus. $E_{sb} = 5,000$ psi
 Element 56 (solid) truss elements 361, 362, 387, 388 (σ_x), 373, 380, 374, 381 (σ_y)

Element	σ_g	Corresponding σ_x, σ_y on solid element	σ_t	σ_{tg}	
361	274.5	47.7	2471.5	2746.0	
362	266.9	47.7	2471.5	2738.4	σ_x
387	240.7	53.1	2751.3	2992.0	
388	233.7	53.1	2751.3	2985.0	
373	347.6	41.5	2150.3	2497.9	
380	213.4	41.5	2150.3	2363.7	σ_y
374	320.	39.7	2057.0	2377.0	
381	196.6	39.7	2057.0	2253.6	

- 2) $E_{sb} = 10,000$ psi

Element	σ_g	Corresponding σ_x, σ_y on solid element	σ_t	σ_{tg}	
361	162.9	11.4	590.7	753.6	
362	164.5	11.4	590.7	755.2	σ_x
387	139.9	17.8	922.3	1062.2	
388	160.8	17.8	922.3	1063.1	
373	230.9	8.9	766.8	997.7	
380	146.2	8.9	766.8	913.0	σ_y
374	211.8	7.9	409.3	621.1	
381	133.8	7.9	409.3	543.1	

3) $E_{sb} = 15,000 \text{ psi}$

Solid elements in compression so no transfer.

Truss element #388 $\sigma_x = 101.9$

Truss element #373 $\sigma_y = 171.9$

4) $E_{sb} = 20,000 \text{ psi}$

No transfer

Truss element #388 $\sigma_x = 80.9$

Truss element #373 $\sigma_y = 136.3$

B. 17-NODE 2" THICK ELEMENTS INTEGRATION ORDER = 4

1) $E_{sb} = 5,000 \text{ psi}$

Element 56 solid. Truss elements 361, 362, 387, 388
 (σ_x) , 373, 380, 374, 381 (σ_y)

Element	σ_g	Corresponding σ_x, σ_y on solid element	σ_t	σ_{tg}	
361	270.7	45.0	2331.6	2602.3	σ_x
362	258.4	45.0	2331.6	2590.0	
387	237.8	42.2	2186.5	2424.3	
388	226.6	42.2	2186.5	2413.1	
373	335.7	36.9	1911.9	2247.6	σ_y
380	214.0	36.9	1914.9	2125.9	
374	309.0	34.0	1761.7	2070.7	
381	196.7	34.0	1761.7	1958.4	

C. 17-NODE 4" THICK ELEMENT (i.e., 2 layers of elements in confined layer)

- 1) $E_{sb} = 5,000$ psi
 Element 19 solid and elements 181, 182, 207, 208 (σ_x);
 elements 193, 200, 194, 201 (σ_y)

Element	σ_g	Corresponding σ_x, σ_y on solid element	σ_t	σ_{ty}	
181	267.6	23.7	1228.0	1495.6	
182	258.8	23.7	1228.0	1486.8	σ_x
207	236.8	36.4	1886.01	2122.8	
208	229.1	36.4	1886.01	2115.1	
193	329.6	16.4	849.7	1179.3	
200	191.1	16.4	849.7	1040.8	
194	306.0	16.0	829.0	1135.0	
207	175.1	16.0	829.0	1004.1	

- 2) $E_{sb} = 10,000$ psi

Element	σ_g	Corresponding σ_x, σ_y on solid element	σ_t	σ_{tg}	
181	159.7	3.6	186.5	346.2	
182	164.0	3.6	186.5	350.5	σ_x
207	138.6	-5.5	285.0	423.4	
208	141.5	5.5	285.0	426.5	
193	273.6	-2.9	--	223.6	
200	139.5	-2.9	--	139.5	
194	206.7	-6.2	--	206.7	
207	126.5	-6.2	--	126.5	

3) $E_{sb} = 15,000 \text{ psi}$

Solid elements in compression at points corresponding to grid.

Max σ_x (el 182) = 122.5 psi

σ_y (el 193) = 168.9 psi

4) $E_{sb} = 20,000 \text{ psi}$

Max σ_x (el 182) = 98.4 psi

σ_y (el 193) = 135.5 psi

D. 8-NODE 1" THICK (i.e., 8 layers of elements in confined layer)

- 1) $E_{sb} = 5,000$ psi
 Element 127 (solid). Truss elements 361, 367 (σ_x), 385,
 388 (σ_y)

Element	σ_g	Corresponding σ_x, σ_y on solid element	σ_t	σ_{tg}	
361	266.7	31.3	1621.8	1888.5	σ_x
367	227.6	57.6	2984.5	3212.1	
385	238.3	40.5	2098.5	2336.8	σ_y
388	220.8	43.0	2228.0	2448.8	

- 2) $E_{sb} = 10,000$ psi

Element	σ_g	Corresponding σ_x, σ_y on solid element	σ_t	σ_{tg}	
361	165.1	-4.2	--	165.1	σ_x
367	136.3	23.5	1217.6	1353.9	
385	158.8	-9.0	466.3	625.1	σ_y
388	147.5	11.0	570.0	717.5	

- 3) $E_{sb} = 15,000$ psi

Element	σ_g	Corresponding σ_x, σ_y on solid element	σ_t	σ_{tg}	
361	120.9	-21.1	--	120.9	σ_x
367	98.1	8.0	414.5	512.6	
385	117.8	-6.5	--	117.8	σ_y
388	109.7	-4.7	--	109.7	

4) $E_{sb} = 20,000 \text{ psi}$

Element	σ_g	Corresponding σ_x, σ_y on solid element	σ_t	σ_{ty}	
361	95.6	-31.1	--	95.6	σ_x
367	76.7	1.0	--	76.7	
385	93.0	-15.8	--	93.0	σ_y
388	86.9	-14.1	--	86.9	

II. ELASTIC LAYER ANALYSIS USING ELSYM5

Stress transfer analysis used composite modulus of 21,515 psi for grid layer, based on

$$E_c V_c = E_s V_s + E_g V_g$$

where

c = composite

s = sand

g = grid

$$\begin{aligned} \text{i.e., } E_c \left(20 \times 8 \times \frac{8}{12}\right) &= 10,000 \left(20 \times 8 \times \frac{8}{12} - 60 \times 11 \times \frac{8}{12} \times \frac{.055}{12}\right) \\ &+ 100,000 \left(60 \times 11 \times \frac{8}{12} \times \frac{.055}{12}\right) \end{aligned}$$

$$106.67 E_c = 20,000(106.67 - 2.017) + 1,000,000(2.017)$$

$$E_c = 21,515 \text{ psi}$$

To transfer,

$$\sigma_g = \frac{\sigma_{\text{tension}}}{V_g / (V_g + V_s)} = \frac{\sigma_t}{0.0189}$$

E_{subbase} (psi)	Max. tensile stress σ_t (psi)	σ_g (psi)
5,000	76.15	4,029.1
10,000	25.07	1323.3
15,000	1.77	93.7
20,000	-11.64	--

Since this is an axisymmetric analysis, $\sigma_x = \sigma_y (= \sigma_g)$